Paleobiology

www.cambridge.org/pab

New insights on metabolic rates and aerobic scopes of the tapejarid pterosaur *Caiuajara dobruskii*

Esaú Victor de Araújo[1,2], Mariana Valeria Haase[3], Jorge Cubo[4], Luiz Carlos Weinschütz[5], Alexander Wilhelm Armin Kellner[1,2] and Juliana Manso Sayão[1,2]

[1]Laboratório de Sistemática e Tafonomia de Vertebrados Fósseis (LAPUG), Departamento de Geologia e Paleontologia, Museu Nacional, Universidade Federal do Rio de Janeiro, Brazil
[2]Programa de Pós-graduação em Zoologia (PPGZoo), Universidade Federal do Rio de Janeiro, Museu Nacional, Brazil
[3]Sorbonne Universite, France
[4]Centre de recherche en paléontologie - Paris - UMR 7207 - CR2P, Sorbonne Université, France
[5]Centro Paleontológico (CENPALEO), Universidade do Contestado, Brazil

Article

Cite this article: Araújo, E. V., M. V. Haase, J. Cubo, L. C. Weinschütz, A. W.A. Kellner, and J. M. Sayão (2026). New insights on metabolic rates and aerobic scopes of the tapejarid pterosaur *Caiuajara dobruskii*. *Paleobiology*, 1–13. https://doi.org/10.1017/pab.2026.10111

Received: 20 August 2025 UTC
Revised: 15 May 2026 UTC
Accepted: 20 May 2026 UTC

Handling Editor:
Catalina Pimiento

Corresponding author:
Esaú Victor de Araújo;
Email: esauvictor13@gmail.com

Abstract

Studies on paleophysiology and thermoregulation are central topics in fossil vertebrate paleobiology because they allow inferences about extinct organismal function beyond anatomical description. Pterosaur thermophysiology remains actively debated. Evidence such as relatively rapid growth and elevated metabolic rate estimates has been used to argue for endothermic-like physiologies consistent with the energetic demands of powered flight, whereas reproductive traits, including burial incubation and precocial development, have led some authors to propose ectothermic strategies more akin to those of extant non-avian diapsids. Here, we provide quantitative estimates of resting metabolic rate (RMR) for the tapejarid pterosaur *Caiuajara dobruskii* using phylogenetic eigenvector maps and osteocyte lacunar density as proxy. Analysis of six histological sections from three appendicular elements (femur, tibia, humerus) at different ontogenetic stages (adult and juvenile) yielded mass-independent RMR estimates of 0.24–0.76 ml O_2 h^{-1} $g^{-0.86}$, substantially higher than those of lepidosaurs but lower than typical mammalian and avian values. The retrodicted mass-independent maximum metabolic rate (MMR) of 5.68 ml O_2 h^{-1} $g^{-0.87}$ falls between values for highly active reptiles and birds, suggesting sufficient aerobic capacity to sustain powered flight without fully matching the maximal performance of small endotherms. Together, these results suggest active-flighted pterosaurs fall among a metabolically intermediate continuum, limiting straightforward actualistic comparisons for inferring their thermoregulatory strategy.

Non-technical Summary

Pterosaurs were flying reptiles that lived alongside dinosaurs and were the first vertebrates to achieve powered flight. How they produced and regulated the heat and energy needed for this lifestyle has been debated for decades, with proposals ranging from reptile-like "cold-blooded" physiology to bird-like "warm-blooded" systems. In this study, bones of the pterosaur *Caiuajara dobruskii* from both juvenile and adult individuals were examined under the microscope. The analysis focused on tiny cavities in the bone that once housed bone cells. The density of these spaces can be used to estimate how rapidly an animal grows, consumes oxygen and, therefore, its metabolic intensity. The results show that *Caiuajara* probably had higher metabolic rates than those of most living reptiles, but not as extreme as those of typical mammals and birds, placing it in an intermediate metabolic continuum. Despite this intermediate metabolism, *Caiuajara* could sustain energetically demanding behaviors, including powered flight, while maintaining a level of internal heat production greater than that of most modern reptiles, though not as intense as in small warm-blooded animals.

Introduction

Thermometabolism is a key dimension of vertebrate evolution, fundamentally shaping physiology, ecology, life history, and the range of achievable metabolic rates (Pettersen et al. 2016). Within amniotes, two main thermogenetic regimes are recognized: endothermy and ectothermy, which differ markedly in both resting and maximal metabolic levels.

Although all animals generate internal metabolic heat, endothermy is defined as relying primarily on this internal heat to maintain stable elevated body temperatures (McNab 2002), often including non-shivering thermogenesis. On the other hand, ectothermy relies predominantly on environmental

PALEOBIOLOGY A PUBLICATION OF THE Paleontological SOCIETY

CAMBRIDGE UNIVERSITY PRESS

heat gained via behavioral and microhabitat adjustments (Clarke and Pörtner 2010; Rowland et al. 2015; Faure-Brac et al. 2022). Consequently, endotherms typically maintain higher and more stable body temperatures and exhibit higher resting and maximum metabolic rates (i.e., oxygen consumption in ml O_2 h^{-1}) compared with ectotherms (Clarke and Pörtner 2010; Faure-Brac et al. 2024).

Extant birds and mammals, the only living endothermic amniotes, are crown representatives of Sauropsida and Synapsida, respectively, having diverged from a common ancestor more than 320 million years ago (Faure-Brac et al. 2024). Within this broader context, several hypotheses propose independent evolutionary pathways to elevated metabolic rates comparable to those of endotherms within Archosauromorpha. Including ancient crocodylomorph lineages (Seymour et al. 2004) and pterosaurs (Clarke and Pörtner 2010), the latter attracting particular attention because their flight-related morphology and life-history traits, suggest the potential for sustained high metabolic performance.

Although the question of pterosaur thermoregulation remains contentious (Kellner and Campos 2002; Unwin and Deeming 2008; Wellnhofer 2008; Clarke and Pörtner 2010), several morphological features provide indirect evidence for elevated metabolic scope in these flying reptiles. Pneumatized bones (Romer 1956; Claessens et al. 2009; Martin and Palmer 2014; Buchmann et al. 2021), elevated growth rates —including prolonged ontogenetic trajectories in taxa such as *Pterodaustro* (Chinsamy et al. 2008) and *Rhamphorhynchus* (Prondvai et al. 2012), and fibrolamellar bone histology (Steel 2008; Araújo et al. 2023) all indicate sustained high rates of bone deposition and, more broadly, elevated physiological performance.

Additional lines of evidence, including broad paleobiogeographic distributions (Kellner et al. 2019a), the evolution of elaborate cranial crests in some taxa (Kellner and Campos 2002; Kellner 2013), the presence of pycnofibers (Kellner et al. 2010; Yang et al. 2019; Cincotta et al. 2022), and complex brain morphology (Edinger 1927, 1941; Hopson 1977; Kellner 1996) have also been interpreted as consistent with elevated levels of physiological activity. However, these inferences are largely qualitative, underscoring the difficulty of reconstructing thermophysiology from fossil remains and motivating more explicitly quantitative approaches.

Among these, quantitative histological proxies provide one of the most direct means of inferring resting metabolic rate (RMR) in extinct vertebrates, as bone-tissue organization records underlying growth dynamics (Padian and Horner 2002; Montes et al. 2007; Cubo and Jalil 2019).

Osteocyte lacunar density has gained prominence in paleophysiological research over the last decade (Cubo et al. 2012). When combined with phylogenetic eigenvector maps (PEMs), these data have been successfully used to infer thermometabolic regimes across terrestrial archosaurs, including *Euparkeria* (Legendre et al. 2013), *Azendohsaurus* sp. (Cubo and Jalil 2019), various pseudosuchians (Legendre et al. 2016; Cubo et al. 2020, 2025; Faure-Brac et al. 2022), and thalattosuchians (Pellarin et al. 2025), as well as in plesiosaurs (Fleischle et al. 2018), synapsids (Faure-Brac and Cubo 2020), and dinosaurs (Bert et al. 2025).

Beyond resting metabolism, maximum metabolic rate (MMR) represents the highest rate at which an organism can consume oxygen to sustain aerobic metabolism during peak activity (Seymour 2013). In extinct taxa, MMR can be estimated using blood flow indices (Q_i) derived from femoral nutrient foramina, which serve as proxies for peak of oxygen consumption (VO_2 max) (Seymour et al. 2012; Hu et al. 2020, 2023; Sena et al. 2025a,b).

When combined with PEM, this approach provides a quantitative framework for reconstructing maximal metabolic performance in extinct clades (Cubo et al. 2025; Pellarin et al. 2025; Sena et al. 2025a,b). Applications to non-avian dinosaurs (Bert et al. 2025), non-mammalian mammaliforms (Newham et al. 2020), non-avian sauropsids (Knaus et al. 2021), extinct birds (Allan et al. 2014), several archosaur groups (Sena et al. 2023, 2025a; Cubo et al. 2025), and a rhamphorhynchid pterosaur (Sena et al. 2025b) demonstrate the potential of these methods for addressing broad questions about vertebrate energetics.

A major constraint for retrodicting RMR and MMR regimes from fossils is the quality of preservation (Cubo et al. 2021). Assemblages preserving three-dimensional (3D) bone architecture are therefore especially informative. The "Cemitério dos Pterossauros" (Pterosaur Graveyard) bonebed from the Upper Cretaceous of southern Brazil represents such an exceptional setting (Kellner et al. 2019b), yielding numerous three-dimensionally preserved specimens of the tapejarid pterosaur *Caiuajara dobruskii* (Manzig et al. 2014).

Recent osteohistological analyses of 18 *Caiuajara* specimens have provided key insights into ontogeny and life history (Araújo et al. 2023), as well as bone laminarity associated with functional biomechanics (Araújo et al. 2025). Together, these data offer a rare opportunity to integrate paleohistological and biomechanical inferences in a single population. Here, a quantitative osteohistological analysis of *C. dobruskii* is presented, constituting a novel application of PEM-based paleophysiological methods to a pterodactyloid pterosaur. As thermometabolism underpins key physiological features linked to biological traits such as growth rates, nutrient and oxygen intake, and locomotion capabilities (Cubo et al. 2025), we estimate both RMR and MMR to quantify aerobic scope and energetic capacity, thereby placing pterosaur thermometabolism within a broader comparative framework.

Materials and Methods

Fossil Material

The analyzed specimens were provided by the Centro Paleontológico da Universidade do Contestado (CENPALEO–UNC) and have been previously described morphologically (Manzig et al. 2014) and histologically (Araújo et al. 2023, 2025). Six osteohistological thin sections were examined: two humeri (CP. V, *CENPALEO–Vertebrados*, catalogue nos. 1032 and 5698), two femora (CP. V 2058 and CP. V 2057), and two tibiae (CP. V 2059 and CP. V 2750a). In addition, a CT-scanned femur (CP. V 8657) was analyzed. All specimens belong to *Caiuajara dobruskii*, a tapejarid pterosaur from the Upper Cretaceous Caiuá Group, Bauru Basin, Brazil (Table 1).

Mid-diaphyseal cross sections of long bones were used to estimate RMR based on osteocyte lacunar density, whereas the CT-segmented femur was used to estimate MMR through analysis of the size of the metaphyseal nutrient foramen.

Osteohistological Procedures

Sampling and thin-section preparation were carried out at the Paleohistology Laboratory of the Department of Geology and Paleontology, National Museum, Rio de Janeiro. All specimens are housed in the same institution. Transverse thin sections of the mid-diaphysis were previously prepared for Araújo et al. (2023) study following established osteohistological methods: bone samples were embedded in clear epoxy resin (Resapol T-208) catalyzed with Butanox M50 (IBEX, Recife, Brazil) and cut using a diamond-tipped blade mounted on a Dremel 3000 saw. The sections were then wet-ground on a metallographic polishing machine (Aropol-E, Arotec Ltda.)

https://doi.org/10.1017/pab.2026.10111 Published online by Cambridge University Press

Table 1. Specimens of *Caiuajara dobruskii* used in this study for metabolic rate estimation. Each element was histologically sampled to estimate resting metabolic rate (RMR) or maximal metabolic rate (MMR), with ontogenetic stages classified as juvenile or adult based on bone microstructure and size (Araújo et al. 2023)

Specimen	Bone element	Ontogenetic Stage	Analysis
CP. V 1032	Humerus	Juvenile	RMR
CP. V 2058	Femur	Juvenile	RMR
CP. V 2059	Tibia	Juvenile	RMR
CP. V 5698	Humerus	Adult	RMR
CP. V 2057	Femur	Adult	RMR
CP. V 2750a	Tibia	Adult	RMR
CP. V 8657	Femur	Adult	MMR

with progressively finer abrasive papers (80/P80, 360/P360, 1200/P1200) until reaching a thickness of approximately 60 µm. Histological structures were examined under a Zeiss Axio Imager.M2 transmitted-light optical microscope equipped with parallel and crossed nicols and fluorescence filters to enhance birefringence, and images were captured using an AxioCam digital camera.

Ontogenetic Control

Specimens were assigned to ontogenetic categories (juvenile, subadult, adult) following the size classes of Manzig et al. (2014) and the osteohistological criteria of Araújo et al. (2023). These criteria include: (1) degree of cortical vascularization; (2) relative abundance of primary versus secondary bone tissue; (3) presence, number, and spacing of lines of arrested growth (LAGs); (4) development of endosteal lamellae and extent of metaphyseal remodeling; and (5) when preserved, degree of fusion of articular ends. Juveniles are characterized by highly vascularized fibrolamellar bone lacking growth marks; subadults by the onset of cortical stabilization and the appearance of the first LAGs; and adults by reduced vascularity, multiple LAGs, and well-developed endosteal lamellae. These ontogenetic categories were explicitly incorporated into the sampling design to assess how metabolic rates vary across the growth series of *C. dobruskii.*

Osteocyte Density

Osteocyte lacunar density was quantified following the protocol described by Cubo et al. (2012), by counting lacunae within the primary bone matrix between primary osteons. Ideally, measurements would be taken from the innermost layers of the primary cortical bone deposited in early ontogeny, as in the original dataset compiled by Cubo et al. (2012). However, extensive bone resorption in the endosteal region resulting from medullary cavity expansion in pterosaur bones (Steel 2008; Eleutério et al. 2015), together with the adult ontogenetic stage of some specimens, precluded sampling of these regions. Consequently, counts were taken from more external regions of the primary cortex, representing the youngest preserved portions of the bone, and osteocyte density was calculated as the number of osteocyte lacunae divided by the analyzed bone area and is expressed as the number of lacunae per square micrometer (µm²).

Phylogenetic Comparative Method and Framework

Phylogenetic relationships among extant taxa were compiled from multiple sources: Neornithes (Bundle et al. 1999; Allan et al. 2014; Stiller et al. 2024); Cetartiodactyla (Zurano et al. 2019); other mammals (Upham et al. 2019; Newham et al. 2020); squamates (Vidal and Hedges 2005; Pyron et al. 2013); and varanid lizards (Villa et al. 2018). Branch lengths for extant taxa were obtained from TimeTree (timetree.org, accessed 29 November 2024), while those for extinct taxa were sourced from the Paleobiology Database (paleobiodb.org, accessed 29 November 2024).

PEMs were generated using the MPSEM (Modelling Phylogenetic Signals using Eigenvector Maps) package (v. 0.6-1; Guénard et al. 2013) in R Studio software (v.2024.12.1 Build 563; R Core Team 2023) to develop regression models for estimating mass-independent RMR and MMR. Alternative models incorporating different co-predictors (plus a null model without co-predictors) were systematically compared using corrected Akaike information criterion (AICc) via forward sequential selection (forward sequential AICc). The osteocyte lacunae density (cell density) model yielded the lowest AICc values and highest adjusted R^2 across skeletal elements (humerus: $R^2 = 0.82$; femur: $R^2 = 0.76$; tibia: $R^2 = 0.99$) and was thus selected as the best-fitting model (detailed model diagnostics reported in "Results"). These models enabled retrodiction of mass-independent RMR and MMR values, along with 95% confidence intervals (CIs), for *C. dobruskii* specimens. Model residuals were assessed for normality using the Shapiro-Wilk test.

Metabolic Rate Retrodictions and Units

RMR To estimate the mass-independent RMR of *C. dobruskii*, we developed phylogenetically informed regression models following the R script and workflow of Legendre et al. (2016). The calibration dataset consisted of measurements from 18 extant amniote species, supplemented here with four additional bird taxa (see Supplementary Table 1), and osteocyte lacunar density from six long bones of *C. dobruskii* (humerus, femur, tibia) was used as the quantitative predictor of mass-independent RMR (Fig. 1). Because osteohistological organization varies among bones, separate comparative datasets were used to fit humeral, femoral, and tibial models (see data.txt used in R analyses in Supplementary Material).

Phylogenetic structure was incorporated using PEM (Guénard et al. 2013), which extends ordinary least squares regression by estimating the strength of phylogenetic signal (α parameter) and including phylogenetic eigenvectors as co-predictors when appropriate. Model fitting followed Guénard et al. (2013), Legendre et al. (2016), and Knaus et al. (2021), and goodness of fit was evaluated using R^2 and AICc, the latter treated descriptively because no alternative model structures were compared. The tibia model showed the best fit ($R^2 = 0.99$; AICc = 3.92), followed by the humerus ($R^2 = 0.82$; AICc = 6.41) and femur ($R^2 = 0.76$; AICc = 17.37), and Shapiro-Wilk tests confirmed that residuals did not deviate from any model. Final PEM models were used to retrodict mass-independent RMR for juvenile and adult *C. dobruskii*, including 95% CIs derived from parametric bootstrapping.

Ancestral Reconstruction of Metabolic Values We reconstructed ancestral RMR for all nodes using the function *fastAnc* from the R package phytools (Revell 2024), following the approach of Faure-Brac and Cubo (2020). This function estimates ancestral states under a Brownian motion model maximum likelihood and provides 95% CIs for each node, which can be visualized directly on the phylogeny.

Because the metabolic values used as input are scaled, dimensionless predictions derived from the PEM models, the reconstructed ancestral states likewise lack physiological units. Accordingly, ancestral character estimation (ACE) results were interpreted in a comparative

https://doi.org/10.1017/pab.2026.10111 Published online by Cambridge University Press

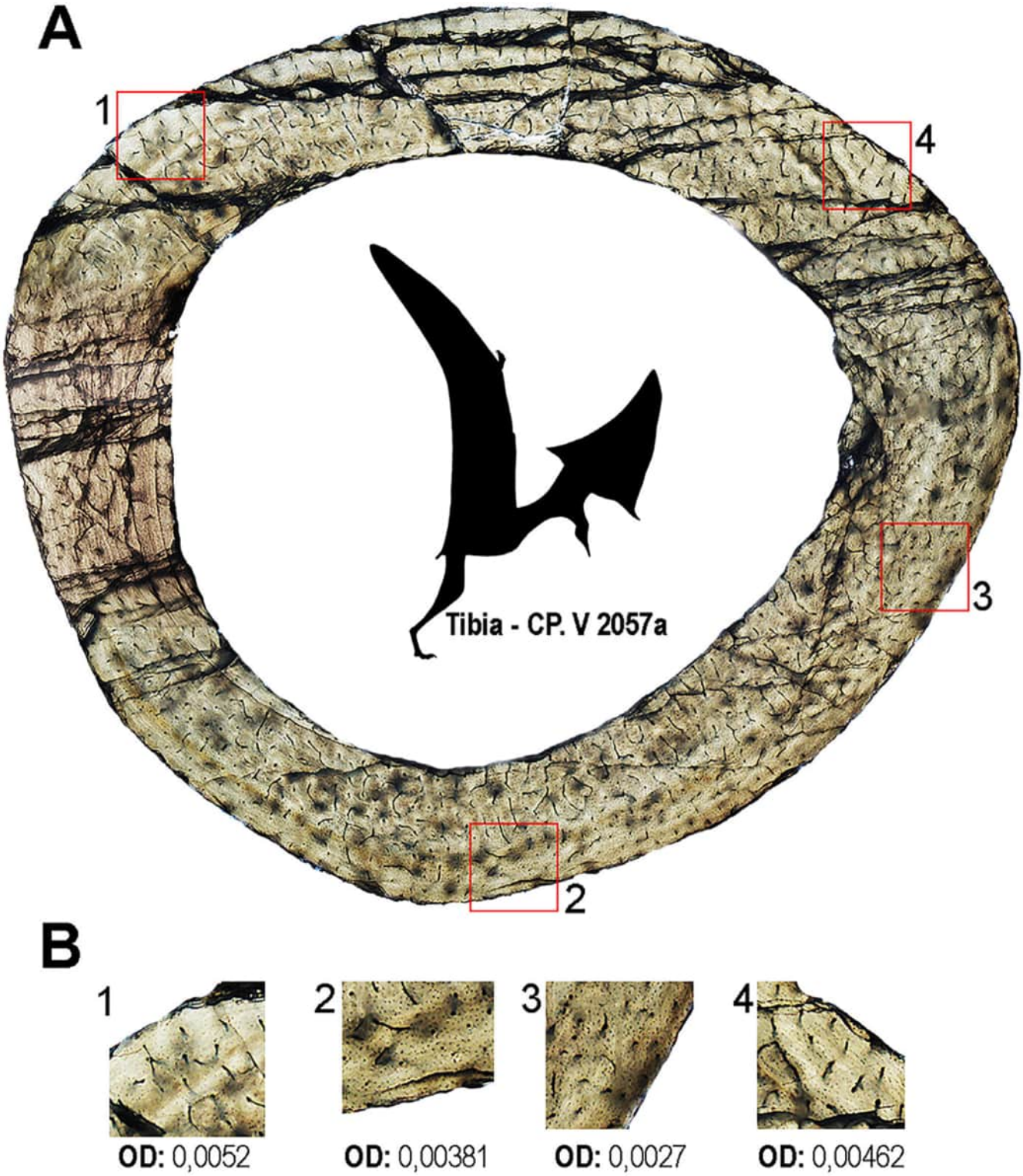

Figure 1. Osteocyte density (OD) as an explanatory factor to infer resting metabolic rate (RMR). **A,** Tibia CP. V 2750a. Marked squares in the cortex indicate regions of the outer cortex delineated by transects. **B,** Transects and respective osteocyte density values obtained.

framework, focusing on the relative phylogenetic position of *C. dobruskii* within the broader metabolic landscape of archosaurs.

MMR We examined 3D models of the *C. dobruskii* femur (CP. V8657). The fossil was scanned using a Zeiss Xradia 510 Versa microtomograph (Zeiss Inc., Barcelona, Spain), equipped with a flat-panel detector, at the National Museum, Federal University of Rio de Janeiro. Segmentation and measurement of the nutrient foramina were performed using Mimics Innovation Suite v. 24 (Materialise) at the Centre de Recherche en Paléontologie–Paris (CR2P). Foramina

https://doi.org/10.1017/pab.2026.10111 Published online by Cambridge University Press

were manually identified using axial scan slices, and 3D rendering was carried out using the Multiple Slice Edit tool. Both the segmentation process and the estimation of the nutrient foramen diameter were conducted using the Mimics software. The measurement protocol involves recording the area of the nutrient foramen as close as possible to the external aperture, to minimize sampling bias between fossil specimens and extant dry bones, whose foramina are typically measured at the bone surface.

The nutrient foramen area on the femur (CP. V 8657) was measured on foramen aperture using ImageJ/Fiji (v. 1.54; Schindelin et al. 2015), approximating the foramen as a geometric circle. Nutrient artery blood flow rate ($\dot{Q}$, in ml s^{-1}) was estimated with the curved polynomial equation: $\log \dot{Q} = -0.20 \log(r_i^2) + 1.91 \log(r_i) + 1.82$ (Seymour et al. 2019), where r_i is the arterial lumen radius derived from the arterial lumen area, assumed to represent roughly 20% of the total foramen area (Hu et al. 2022).

To estimate the mass-independent MMR for the femur (CP. V 8657), we applied a phylogenetic inference model based on femoral nutrient foramina data (Fig. 2). Our extant dataset comprised MMRs, body masses, and nutrient artery blood flow ($\dot{Q}$) values from 43 amniote species, including 15 mammals, 14 non-avian sauropsids, and 14 avian sauropsids (see Supplementary Table 2). This approach allowed us to infer the mass-independent MMR from femoral nutrient foramen data.

Allometric Correction and Metabolic Units Some authors have shown that the MMR is corrected with different mass exponents depending on the clade. For example, in mammals, the mass exponent is 0.870, higher than in sauropsids corresponding to 0.829 (mass-independent MMR (White and Seymour 2005; Seymour 2013; Hu et al. 2022). To correct the allometric effects (i.e., the increasing surface-to-volume ratio with decreasing mass), we applied phylogenetic exponents in our analyses of 0.86 for RMR and 0.87 for MMR. These values correspond to the phylogenetic means recovered using Mesquite (Maddison and Maddison 2016) according to the different dataset for each analysis. This generates a single character matrix of distinct extant species exponents: 0.829 for non-avian sauropsids (Seymour 2013), 0.87 for synapsids (White and Seymour 2005), and 1.02 for avian species (Allan et al. 2014), and a question mark for fossil taxa using the *Reconstruct ancestral states* function with the Character History Source option in the Trace. Consequently, the mass-independent RMR unit is expressed in ml O_2 h^{-1} $g^{-0.86}$ and the mass-independent MMR unit in ml O_2 h^{-1} $g^{-0.87}$.

Results

Adult and Juvenile Caiuajara dobruskii *RMR Retrodiction*

Mass-independent RMR estimates for juvenile and adult *C. dobruskii* were broadly similar across skeletal elements (Table 2). The phylogenetic eigenvector-based regression models used for RMR retrodiction demonstrated strong explanatory power: for the humerus and femur models, R^2 values were 0.82 and 0.76, respectively, whereas the tibial model exhibited exceptionally high performance ($R^2 = 0.99$; AICc = 3.92). No alternative models provided a better fit based on AICc comparisons, and therefore model selection was not required (see "Materials and Methods"). For the humerus, the retrodicted mass-independent RMR was 0.70 (95% CI: 0.49–1.02) ml O_2 h^{-1} $g^{-0.86}$ in the juvenile and 0.60 (95% CI: 0.42–0.86) ml O_2 h^{-1} $g^{-0.86}$ in the adult. The tibial models produced the lowest values, 0.18 (95% CI: 0.11–0.29) ml O_2 h^{-1} $g^{-0.86}$ in the adult and 0.15 (95% CI: 0.09–0.23) ml O_2 h^{-1} $g^{-0.86}$ in the juvenile (Fig. 3). Femoral retrodictions were intermediate,

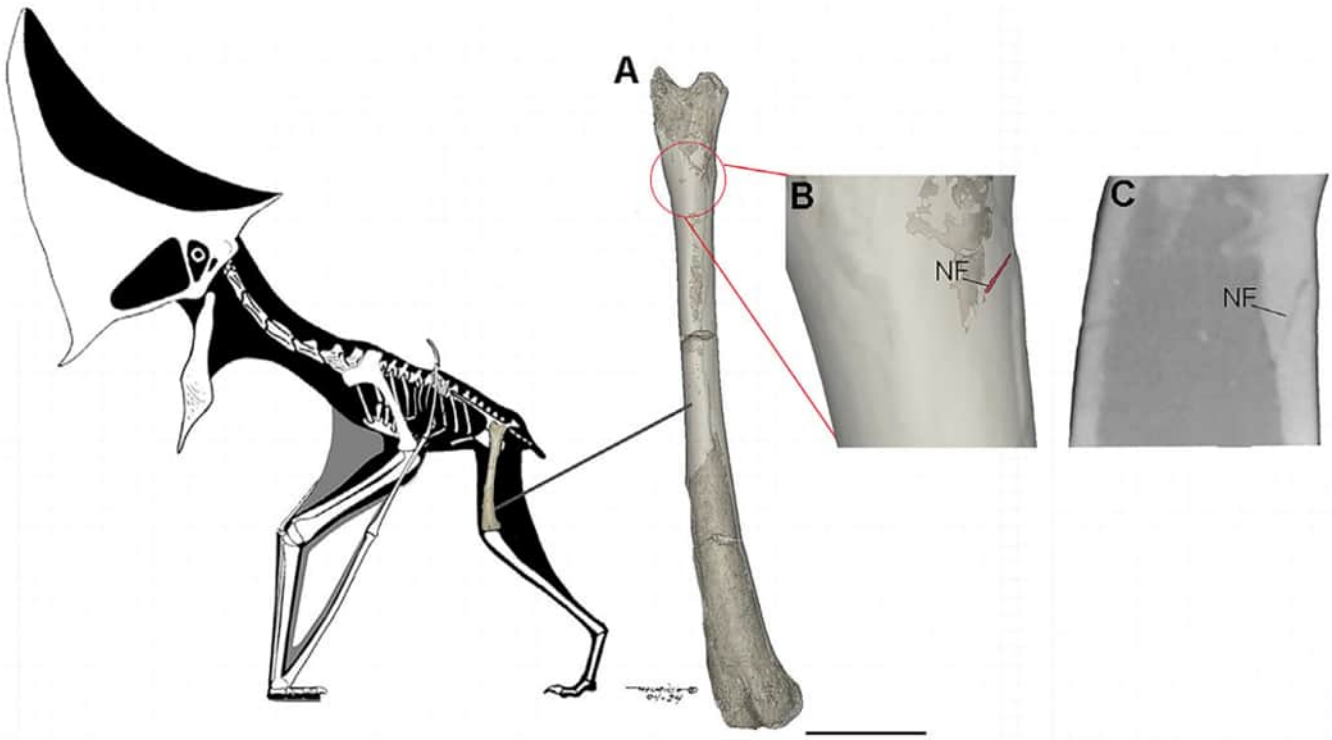

Figure 2. Mass-independent maximum metabolic rate (MMR) inferred using metaphyseal femoral nutrient foramen measurements. **A,** CT image of a *Caiuajara dobruskii* femur (CP. V 8657), showing the nutrient foramen region in metaphysis. B and C, Close-up views of the nutrient foramen (NF) from CT scans. Scale bar equals 5 cm (A).

https://doi.org/10.1017/pab.2026.10111 Published online by Cambridge University Press

Table 2. *Caiuajara dobruskii* resting metabolic rate (RMR) values calculated in this study using data available from literature

Specimen	Bone	Ontogenetic stage	RMR (ml O_2 h^{-1} $g^{-0.86}$)
CP. V 2058	Femur	Adult	0.24
CP. V 2057	Femur	Juvenile	0.26
CP. V 2059	Tibia	Juvenile	0.76
CP. V 2750a	Tibia	Adult	0.63
CP. V 1032	Humerus	Juvenile	0.70
CP. V 5698	Humerus	Adult	0.60

yielding 0.22 (95% CI: 0.13–0.36) ml O_2 h^{-1} $g^{-0.86}$ in juveniles and 0.30 (95% CI: 0.19–0.48) ml O_2 h^{-1} $g^{-0.86}$ in adults.

Statistical Comparison to Extant Taxa

The estimated RMR of *C. dobruskii* femur PEM: 0.22–0.36 (central: 0.285) yields a *z*-score of +5.15 relative to ectotherms (mean = 0.079, SD = 0.040; $n = 10$) and −1.53 relative to endotherms (mean = 1.96, SD = 1.11; $n = 12$), positioning it as a statistical extreme outlier in the ectothermic spectrum (5.2 SD above mean) but well within the physiological variation of endotherms (1.5 SD below mean; Supplementary Fig. 1).

Reconstruction of Ancestral RMR Values across Phylogeny

Ancestral reconstruction of RMR under a maximum-likelihood framework reveals a clear phylogenetic gradient. Basal nodes exhibit low reconstructed values (ranging approximately from −2.8 to −2.0), whereas progressively higher values are observed toward more derived clades, reaching up to about 0.77 in terminal nodes (Fig. 4).

The analyzed fossil taxon falls within this upper range, aligning with the elevated values characteristic of derived nodes and clearly differing from the lower estimates reconstructed for basal ancestors. Overall, the pattern indicates a continuous evolutionary gradient in reconstructed values throughout phylogeny, with marked differences between deep ancestral nodes and more derived taxa.

Adult Caiuajara dobruskii *MMR Retrodiction*

The retrodicted mass-independent MMR for *C. dobruskii* was 5.68 (95% CI: 4.66–7.74) ml O_2 h^{-1} $g^{-0.87}$, with estimated femoral blood flow (Q) serving as a co-predictor in the phylogenetic regression model ($R^2 = 0.90$; corrected Akaike information criterion, AICc = 58.28; $p = 5.50 \times 10^{-12}$; Fig. 5). This mass-independent MMR lies above typical values reported for extant ectothermic reptiles (< 1 ml O_2 h^{-1} $g^{-0.87}$) and overlaps the lower range of birds and other high-performance vertebrates, indicating a substantially elevated aerobic capacity relative to ectotherms while remaining below the highest values observed in mammals.

Discussion

RMR Estimates across Major Clades

Our quantitative analyses retrodicted mass-independent RMR values for *Caiuajara dobruskii* ranging from 0.24 to 0.76 ml O_2 h^{-1} $g^{-0.86}$. These values are substantially higher than those typically observed in extant ectothermic sauropsids (0.03–0.15 ml

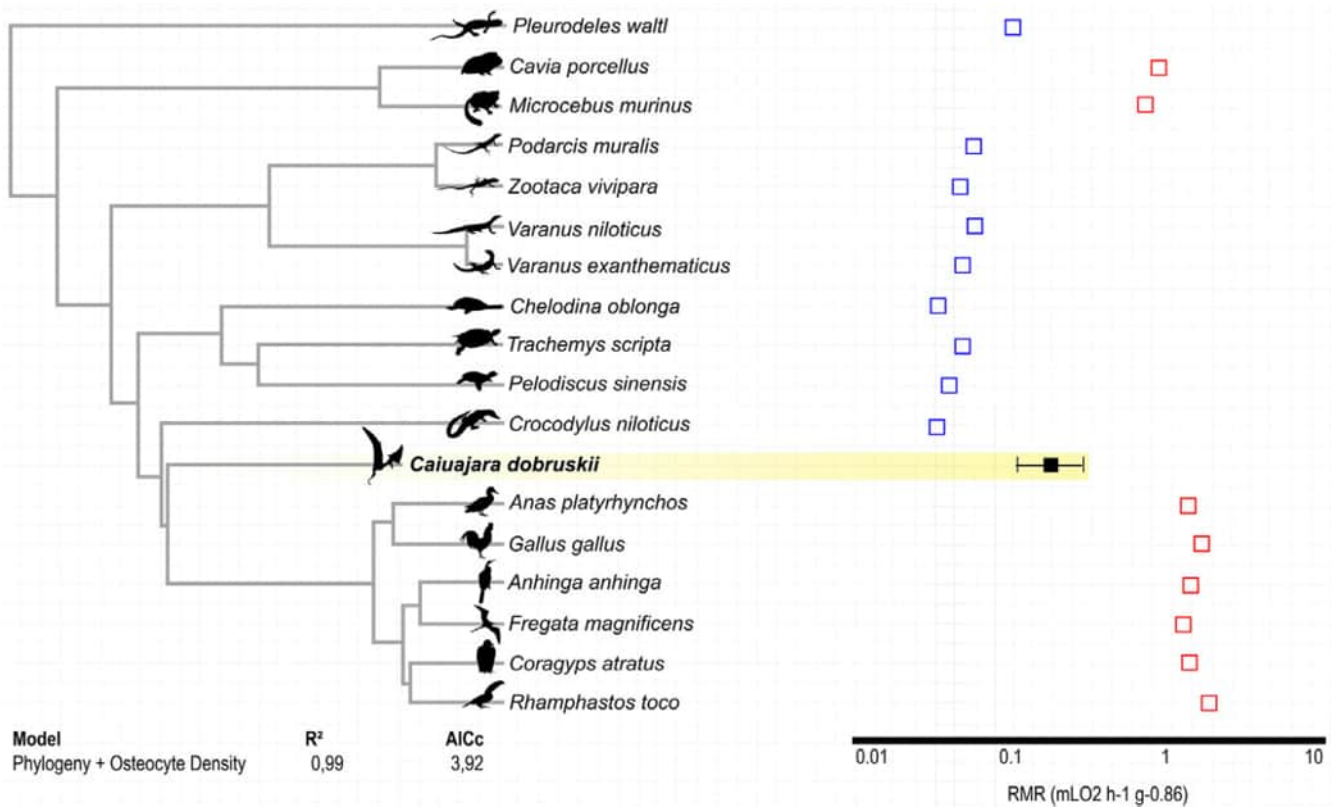

Figure 3. Results of the phylogenetic eigenvector map (PEM) analysis using osteocyte density as predictor variable for mass-independent resting metabolic rate (RMR) inferences in ml O_2 h^{-1} $g^{-0.86}$. Dark blue squares represent ectotherms, while red squares denote endotherms. Black square represents the mass-independent RMR values of *Caiuajara dobruskii*.

https://doi.org/10.1017/pab.2026.10111 Published online by Cambridge University Press

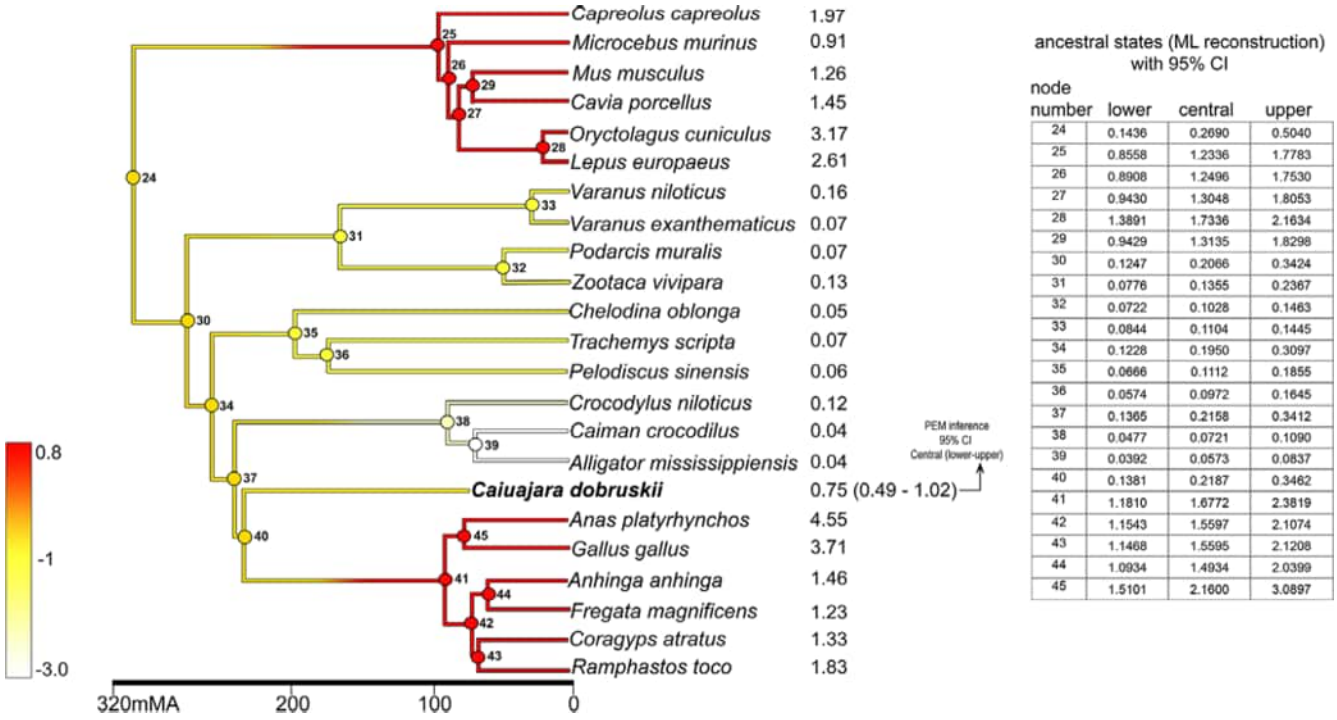

node number	lower	central	upper
24	0.1436	0.2690	0.5040
25	0.8558	1.2336	1.7783
26	0.8908	1.2496	1.7530
27	0.9430	1.3048	1.8053
28	1.3891	1.7336	2.1634
29	0.9429	1.3135	1.8298
30	0.1247	0.2066	0.3424
31	0.0776	0.1355	0.2367
32	0.0722	0.1028	0.1463
33	0.0844	0.1104	0.1445
34	0.1228	0.1950	0.3097
35	0.0666	0.1112	0.1855
36	0.0574	0.0972	0.1645
37	0.1365	0.2158	0.3412
38	0.0477	0.0721	0.1090
39	0.0392	0.0573	0.0837
40	0.1381	0.2187	0.3462
41	1.1810	1.6772	2.3819
42	1.1543	1.5597	2.1074
43	1.1468	1.5595	2.1208
44	1.0934	1.4934	2.0399
45	1.5101	2.1600	3.0897

Figure 4. Maximum-likelihood (ML) ancestral state reconstruction of mass-independent resting metabolic rate (RMR) across extant amniotes and *Caiuajara dobruskii*, based on values inferred with phylogenetic eigenvector maps (PEMs) for the fossil taxon and measured by respirometry for living species (units in ml O_2 h^{-1} $g^{-0.86}$). Branch colors represent reconstructed RMR values along the phylogeny, from low (yellow) to high (red), and numbered internal nodes correspond to ML ancestral estimates summarized in the adjacent table, which reports central values and 95% confidence intervals (CIs). Within Archosauria, basal nodes exhibit low reconstructed RMR compatible with plesiomorphic ectothermy, whereas more derived ornithodiran nodes show progressively elevated values, with *C. dobruskii* plotting among the highest ancestral estimates, close to those of modern birds.

O_2 h^{-1} $g^{-0.86}$; mean ≈ 0.07; e.g., *Alligator mississippiensis*, *Caiman crocodilus*, *Varanus niloticus*; Fleischle et al. 2018; Sena et al. 2023; Pellarin et al. 2025), yet considerably lower than those of modern endotherms such as birds and mammals (1.25–4.54 ml O_2 h^{-1} $g^{-0.86}$; mean ≈ 2.5). Accordingly, the estimated RMR of *C. dobruskii* is approximately 4- to 12-fold higher than the ectothermic mean, but 3- to 6-fold lower than that of typical endotherms.

Using the central estimate derived from the femur PEM (0.285 ml O_2 h^{-1} $g^{-0.86}$) yielded a *z*-score of +5.15 for *C. dobruskii* relative to ectotherms (mean = 0.079, SD = 0.040; $n = 10$) and −1.53 relative to endotherms (mean = 1.96, SD = 1.11; $n = 12$). This places it as an extreme statistical outlier among ectotherms (more than 5 SD above the mean), while remaining within the range of endothermic variation (1.5 SD below the mean; Supplementary Fig. 1). Importantly, 95% CIs of our estimates do not overlap with those of either sampled ectotherms or endotherms.

Taken together, these results position *C. dobruskii* within a quantitatively intermediate metabolic continuum relative to extant tetrapods. This pattern is further supported by estimated mass-independent MMR values, which fall between those highly active ectothermic reptiles (e.g., varanids) and those of birds and mammals, indicating an overall metabolic regime elevated above typical ectothermy, yet not reaching the full intensity of endothermy.

Comparative biological evidence reinforces the plausibility of such intermediate metabolic strategies. In fishes, regional endothermy has evolved independently in tunas (Ciezarek et al. 2019), billfish (Istiophoridae and Xiphiidae), and lamnid sharks (Lamnidae; Pimiento et al. 2019), demonstrating that elevated aerobic performance and increased tissue temperatures can arise through distinct physiological and evolutionary pathways (Block et al. 2011). Similarly, leatherback sea turtles (e.g., *Dermochelys coriacea*) elevate their internal body temperatures above ambient conditions through increased metabolic activity, without maintaining strict homeothermy (Paladino et al. 1990; Dawson et al. 2020). These examples indicate that intermediate metabolic states are not anomalous, but rather part of a broader physiological continuum.

Histological evidence further supports this interpretation by revealing heterogeneity in growth dynamics among pterosaurs. For instance, *Pterodaustro* exhibits an initial phase of rapid growth lasting approximately 2 years, followed by 3 to 4 years of slower bone deposition, indicating a determinate and prolonged ontogeny (Chinsamy et al. 2008). In contrast, *Rhamphorhynchus* displays a more gradual and continuous growth pattern, suggesting greater ontogenetic plasticity and potentially more moderate metabolic rates (Prondvai et al. 2012). *Caiuajara*, in turn, appears to have sustained elevated growth rates throughout ontogeny, without clear development of parallel-fibered bone associated with the onset of flight (Araújo et al. 2023), which may indicate a more persistently elevated physiological regime.

Within a broader macroevolutionary context, reconstructed RMR values across Archosauria indicate a directional trend from low values at basal nodes toward progressively higher metabolic levels in more derived lineages (Grigg et al. 2022). This pattern suggests that elevated aerobic capacity and enhanced thermoregulatory potential began to emerge early in archosaur evolution, rather than arising abruptly in crown groups. The metabolic position of *Caiuajara* within this gradient reinforces this interpretation: its estimated RMR aligns with elevated values observed in derived nodes, indicating a level of energetic performance well above plesiomorphic ectothermy.

https://doi.org/10.1017/pab.2026.10111 Published online by Cambridge University Press

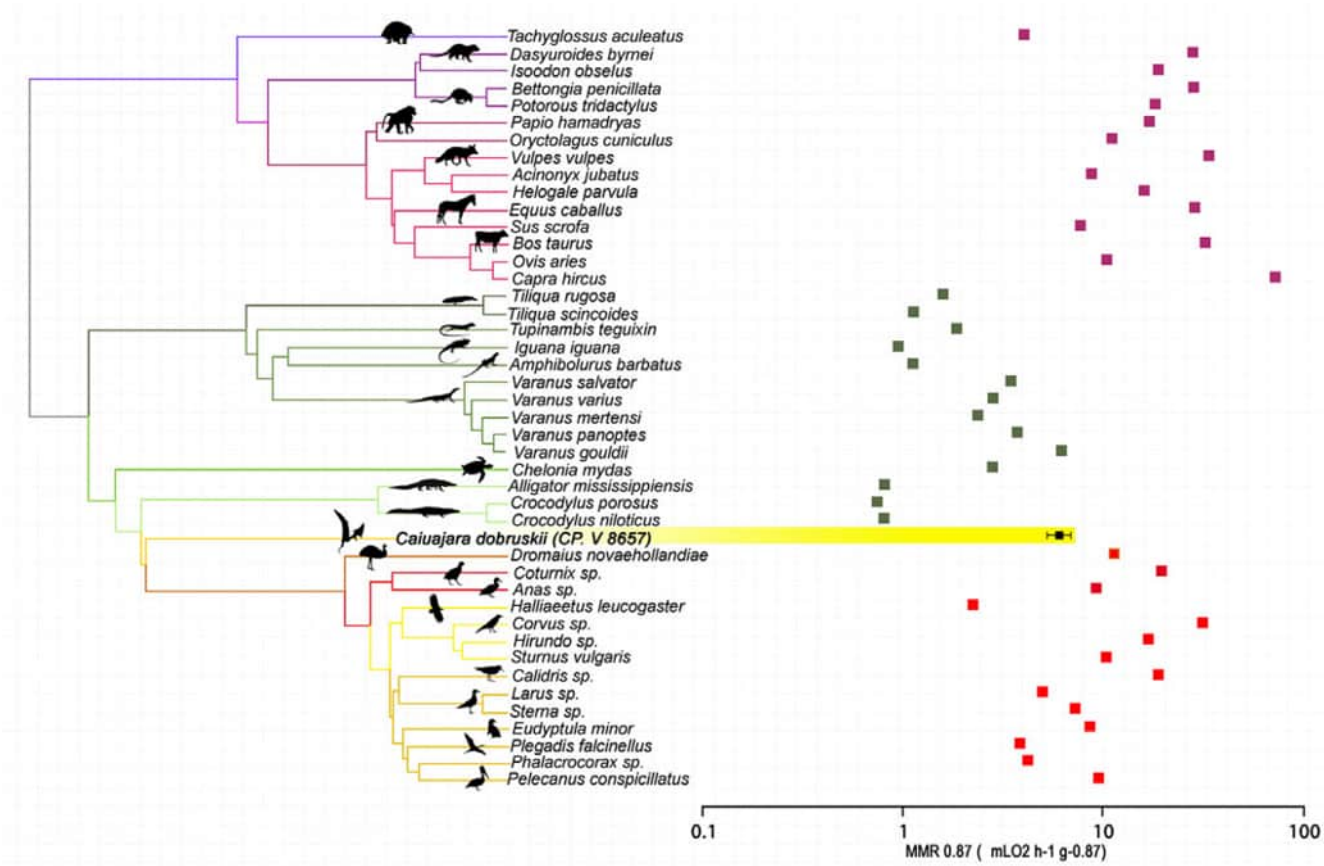

Figure 5. Phylogenetic eigenvector map (PEM) including a sample of extant amniotes used to construct the mass-independent maximal metabolic rate (MMR) inference model. Retrodictions for pterosaurs were performed using the nutrient artery $Q^{\cdot}$value as a co-predictor. Pink squares represent MMR values measured for Synapsida; dark green squares indicate values observed in non-avian sauropsids; red squares correspond to MMR values observed in birds; and the black square represents the fossil taxon *Caiuajara dobruskii.*

This evolutionary framework suggests that increases in activity, growth rate, and metabolic intensity were tightly linked during archosaur diversification. In pterosaurs, the origin of powered flight likely imposed substantial energetic demands and may have favored the evolution of elevated metabolic performance, without requiring physiological equivalence to the thermoregulatory regimes of extant birds or mammals (Mozo et al. 2005).

Accordingly, our results support the presence of intermediate metabolic conditions in *C. dobruskii*, reflecting its position within a broader evolutionary continuum of increasing metabolic intensity, without implying a single, intermediate discrete thermoregulatory strategy.

On the Use of "Mesothermy" and Intermediate Metabolic States

The term "mesothermy" has been widely used to describe organisms that exhibit metabolic rates intermediate between those of ectotherms and endotherms (Grady et al. 2014). In this context, the position of *C. dobruskii* within a quantitatively intermediate metabolic continuum is broadly consistent with the "mesothermic" condition inferred for non-avian dinosaurs based on growth scaling (Grady et al. 2014) and for basal archosauromorphs using phylogenetic eigenvector mapping approaches (Legendre et al. 2016).

However, this classification should be treated with caution. As emphasized by Legendre et al. (2016), intermediate metabolic rates may reflect an evolutionary gradient of ancestrally elevated metabolic levels within Archosauromorpha, rather than a discrete thermoregulatory category.

Given these considerations, we interpret the metabolic profile of *C. dobruskii* as part of a broader continuum of intermediate physiological states, characterized by RMR and MMR that exceed those of most extant ectotherms but do not match the full intensity observed in typical endotherms. In this sense, *Caiuajara* may be described as metabolically intermediate and broadly compatible with mesothermy *sensu lato*, understood here as a descriptive term for taxa showing intermediate metabolic intensity and partial thermoregulatory capacity. Importantly, comparable physiological patterns occur in a variety of extant vertebrates, including highly active taxa with ectothermic ancestry, such as tunas and lamnid sharks, as well as lineages with endothermic ancestry but reduced metabolic intensity, such as monotremes. These examples indicate that intermediate metabolic regimes can arise through multiple physiological and evolutionary pathways and should not be taken to imply a single underlying mechanism or a strictly defined thermoregulatory category. Accordingly, the metabolic pattern inferred for *C. dobruskii* is best viewed as consistent with a spectrum of intermediate physiological conditions, rather than as evidence for one exclusive thermoregulatory strategy. In the absence of direct physiological data, we therefore refrain from assigning *Caiuajara* to a rigid categorical framework and instead emphasize its position within a metabolically intermediate continuum.

Importantly, the combination of moderately elevated RMR and relatively high estimated MMR suggests that *Caiuajara* possessed

https://doi.org/10.1017/pab.2026.10111 Published online by Cambridge University Press

the capacity for energetically demanding behaviors, such as sustained flight, while likely exhibiting limited or partial thermal stability. This provides a plausible physiological explanation for its intermediate position relative to extant ectotherms and endotherms, while explicitly acknowledging that multiple thermoregulatory scenarios, including mesothermy *sensu lato*, remain plausible.

Finally, because no sampled extant tetrapod exhibits a comparable combination of traits—and given the absence of direct living analogues for pterosaurs, straightforward actualistic comparisons are not possible for this taxon. Accordingly, any metabolic classification should be treated with caution. Nevertheless, this study represents one of the first quantitative efforts to reconstruct RMR and MMR in pterosaurs, contributing to a more refined understanding of the physiology of these remarkable flying reptiles.

Ontogenetic Patterns and Functional Implications

Across ontogeny, both juvenile and adult specimens of *C. dobruskii* exhibit relatively high mass-independent RMR values. Juvenile humeri yield slightly higher retrodicted rates, consistent with the elevated energetic requirements of rapid skeletal growth and active thermoregulation during early life stages (Glazier 2005; Araújo et al. 2023). However, unexpected patterns were detected in the femur and tibia, where RMR values were higher in adults than in juveniles.

In taxa reliant on terrestrial or saltatory locomotion, cortical ossification often intensifies during later developmental stages, leading to an increase in osteocyte lacunae density and, consequently, higher inferred RMR values (Huttenlocker and Farmer 2017; Cubo et al. 2025). In *C. dobruskii*, this pattern may reflect ontogenetic shifts in hindlimb function, potentially linked to changes in locomotor behavior or the increasing structural demands of takeoff and landing. These findings suggest that pterosaur bone physiology was highly dynamic, with metabolic and biomechanical demands changing during development in response to functional constraints.

In vertebrates, MMR is tightly coupled with circulatory efficiency, as increasing metabolic and locomotor demands require enhanced oxygen delivery. One reliable proxy used to estimate MMR in extinct taxa is the size of the nutrient foramina in long bones, particularly in the femur, as this reflects the capacity of the nutrient artery to supply oxygenated blood to bone tissue (Seymour et al. 2012, 2019; Hu et al. 2018). In extant terrestrial vertebrates, species that exhibit higher locomotor activity possess relatively larger nutrient foramina, indicating a greater demand for oxygen to support bone remodeling and repair (Bishop and Butler 1995; Bundle et al. 1999; Allan et al. 2014). Moreover, the biomechanical stresses associated with high activity levels often lead to microfractures, necessitating increased bone remodeling and further oxygen consumption (Seymour 2013).

For an adult *C. dobruskii*, mass-independent MMR was retrodicted to be 5.68 ml O_2 h^{-1} $g^{-0.87}$, a value overlapping the lower range of modern birds, which present mass-independent MMR in the range 4–10 ml O_2 h^{-1} $g^{-0.87}$ (Bundle et al. 1999; Seymour et al. 2019; Hu et al. 2021). This high metabolic capacity is critical for sustaining powered flight, as it ensures a continuous energy supply and efficient aerobic metabolism. In contrast, extant ectothermic reptiles, such as lizards, typically have mass-independent MMR values <1 ml O_2 h^{-1} $g^{-0.87}$ (Bennett and Ruben 1979). The overlap between the estimated MMR of *C. dobruskii* and the lower avian range reinforces the notion that these pterosaurs were capable of energetically demanding activities, including sustained flight, and required a highly efficient aerobic system. As our MMR retrodictions were based solely on adult specimens, future analyses of immature individuals will be crucial to fully understand metabolic scaling across ontogeny.

Notably, this estimate closely matches the mass-independent MMR 5.55 ml O_2 h^{-1} $g^{-0.87}$ (95% CI: 4.37–7.05) recently estimated for a juvenile *Rhamphorhynchus* using the same femoral nutrient foramen methodology (Sena et al. 2025b). Despite major differences in body size (long-tailed non-pterodactyloid vs. short-tailed pterodactyloid), wing architecture, and paleoecology (Jurassic lagoon piscivore vs. Cretaceous desert inhabitant), both taxa converge on comparable maximal aerobic capacities that overlap the lower range of modern birds and exceed typical ectothermic reptiles by more than fivefold. This metabolic equivalence across Pterosauria lineages suggests that high aerobic performance constituted a fundamental ornithodiran adaptation for powered flight, potentially enabling sustained aerial locomotion irrespective of specific biomechanical or ontogenetic constraints.

Further, while these findings suggest a physiological convergence between pterosaurs and birds, high metabolic rates in *C. dobruskii* may not be solely the result of ecological adaptations. Our ACE analyses reveal a strong phylogenetic structuring of metabolic traits: basal archosaur nodes exhibit markedly low reconstructed mass-independent RMR values (approximately −2.8 to −2.0), whereas more derived ornithodiran nodes show a progressive rise, reaching positive values up to ~0.7. *Caiuajara dobruskii* plots within this upper range of derived nodes, indicating that its elevated metabolic rate is consistent with, rather than exceptional relative to, the metabolic landscape inherited from advanced ornithodiran ancestors. This pattern suggests that part of its metabolic physiology reflects phylogenetic inertia rather than pure ecological innovation.

However, the apparent overlap between the upper range of inferred reptilian MMR and the lower range of avian values in our dataset is driven primarily by varanid lizards, which are highly active squamates that can attain aerobic metabolic rates comparable to those of small mammals, although this elevated condition is not maintained continuously (Thompson and Withers 1997; Frappell and Butler 2004; Clemente et al. 2009). These reptiles also possess disproportionately large femoral nutrient foramina relative to most other ectotherms (Seymour et al. 2012; Varela et al. 2024). Because our MMR estimates are derived from this osteological proxy rather than from direct respirometry, they likely reflect a combination of genuine convergence in bone perfusion and activity levels and methodological scatter and therefore should be interpreted as indicating broad energetic capacities rather than implying equivalent whole-organism performance between reptiles and birds.

Similarly, the MMR retrodiction of *C. dobruskii* aligns with the higher energetic capacity characteristic of derived archosaurs, reinforcing the interpretation that both its resting and maximal metabolic traits represent an elevated, intermediate metabolic condition arising from a combination of inherited high-performance physiological baselines and ecological demands associated with powered flight.

Ecological and Behavioral Implications

The *Caiuajara* assemblage was discovered in a sand sea formed within an interior paleodesert (Manzig et al. 2014). In such harsh environments, animals must contend with extreme daytime heat and markedly lower nighttime temperatures (Williams and Tieleman 2005). The relatively high RMR observed in juvenile

https://doi.org/10.1017/pab.2026.10111 Published online by Cambridge University Press

C. dobruskii, while only marginally higher than adult values, suggests that these pterosaurs likely exhibited some degree of thermoregulatory control despite their increased vulnerability to thermal fluctuations. Juveniles are likely to face higher energetic demands associated with maintaining thermal balance under these challenging conditions.

The large premaxillary crest in tapejarid pterosaurs has been proposed to contribute to thermoregulation (Kellner and Campos 2002; Kellner 2013). However, the crest in *C. dobruskii* is only fully developed in adults, while RMR values were similar across ontogenetic stages. This pattern implies that the crest likely had a minimal role in thermoregulation in *Caiuajara* and was instead linked to sexual maturity. Such a developmental pattern supports hypotheses that these prominent cranial structures primarily functioned in visual communication, social signaling, and hierarchy establishment—roles that become particularly important once reproductive maturity is reached. Ontogenetic studies of related tapejarids (Vullo et al. 2012; Naish et al. 2021; Zhou et al. 2022) further reinforce the idea that crest development is more closely associated with maturity than with physiological regulation. Similar display structures in both extant and extinct taxa often serve comparable roles in intra- and interspecific interactions (Evans 2006; Gates et al. 2016; DeSantis et al. 2020; Torres et al. 2025).

The overrepresentation of juveniles in the *Caiuajara* assemblage has spurred several hypotheses regarding their depositional dynamics. One possibility is that a "creching" behavior—akin to that observed in modern birds (Araújo et al. 2023) may have facilitated group aggregation during reproductive periods, thereby enhancing protection and thermoregulation. In extant colonial birds such as flamingos (Phoenicopteridae) (Pickering et al. 1992), pelicans (Pelecanidae) (Evans 1984), and penguins (Spheniscidae) (Handrich et al. 1997), creching is vital for minimizing heat loss and maintaining stable body temperatures, particularly under extreme environmental conditions. Similarly, the increased sensitivity of *Caiuajara* juveniles to temperature fluctuations may have favored such social and behavioral strategies for thermoregulation, particularly during the cooler desert nights (Fernandes and Magalhães-Ribeiro 2015). These parallels with modern avian taxa underscore the possibility that pterosaurs employed complex physiological and behavioral adaptations to cope with their environment.

Moreover, the retrodicted mass-independent RMR values for *C. dobruskii* (0.24–0.76 ml O_2 h^{-1} $g^{-0.86}$) fall between the typical ranges of modern ectotherms and endotherms, with confidence intervals that exclude both groups. In contrast, the estimated mass-independent MMR suggests a high aerobic capacity compatible with powered flight. These histologically derived estimates, normalized by a phylogenetic body-mass exponent, represent the first direct RMR retrodictions in pterosaurs and indicate that *Caiuajara* occupied an intermediate metabolic continuum, rather than matching any extant ectothermic or endothermic pattern. Given the lack of living tetrapods with this specific combination of resting and maximal metabolic rates, we refrain from inferring a single, definitive thermoregulatory strategy for *Caiuajara* and instead emphasize its placement within a continuum of intermediate metabolic conditions. Nonetheless, because the present study is based solely on *C. dobruskii*, further research across a broader range of pterosaur taxa will be essential to determine whether this metabolic pattern was widespread within the clade. Future investigations should aim to expand the sample size of both pterosaurs and extant taxa, especially birds, thereby enabling broader generalizations regarding pterosaur metabolic physiology and its ecological and evolutionary implications.

Conclusions

This study presents the first quantitative retrodictions of mass-independent RMR and MMR for *Caiuajara dobruskii*, providing new insights into pterosaur metabolic scope and thermophysiology. The reconstructed RMR values place *C. dobruskii* clearly above ectothermic sauropsids yet well below the mean of modern endotherms, indicating a metabolically intermediate continuum broadly compatible with mesothermy *sensu lato*. Both juvenile and adult specimens exhibit similar intermediate RMR values throughout ontogeny, although shifts in bone physiology may reflect changes in locomotor performance and functional demands. A mass-independent MMR estimate of 5.68 ml O_2 h^{-1} $g^{-0.87}$ places *C. dobruskii* within the metabolic range of highly active reptiles, such as varanids, while overlapping with values reported for some modern birds and small mammals. Together, these results suggest that *C. dobruskii* possessed a well-developed aerobic system capable of sustaining energetically demanding behaviors, including prolonged powered flight, although likely without reaching the extreme performance levels of small endotherms. Combined RMR and MMR estimates indicate that *C. dobruskii* occupied an intermediate position within a broader metabolic continuum between typical ectothermic reptiles and fully endothermic birds and mammals, without uniquely resolving its thermoregulatory strategy. Furthermore, the apparent lack of a thermoregulatory function for the cranial crest, combined with its delayed development, supports a sociosexual signaling role rather than physiological regulation. Behavioral adaptations such as possible creching behavior may have mitigated thermal stress in juvenile aggregations, particularly under extreme desert conditions. Broader taxonomic sampling of both pterosaurs and extant analogs, utilizing specimens from other pterosaur bonebeds such as *Hamipterus tianshanensis* and *Pterodaustro guinazui*, will be essential to evaluate how widespread such metabolic conditions were across Pterosauria.

Acknowledgments. E.V.A. acknowledges the Programa de Pós-Graduação em Zoologia (PPGZoo) for their grant support, as well as Center for Research on Palaeontology–Paris (CR2P)–Sorbonne University for the internship that contributed to this research. This study was funded by the Conselho Nacional de Desenvolvimento Científico e Tecnológico (CNPq: 141138/2022-0 to E.V.A; 309245/2023-0, 408309/2025-3 to J.M.S; and 308707/2023-0, and 406902/2022-4–INCT PALEOVERT to A.W.A.K.), and Fundação de Amparo à Pesquisa do Estado do Rio de Janeiro (FAPERJ: E-26/200.558/2026E-26/201.095/2022 to A.W.A.K.; E-26/210.066/2023 and E-26/210.734/2024 to J.M.S). This project received funding from the European Union's Horizon 2020 research and innovation programme under the Marie Skłodowska-Curie grant agreement 101107135 to M.V.H. Also, the authors thank M. A. Raposo and R. Stopiglia (Setor de Ornitologia, Museu Nacional/UFRJ) for bird sample curatorial assistance and I. Rocha for technical support with 3D segmentation.

Author Contribution. E.V.A.: Conceptualization; data curation; formal analysis; investigation; methodology; writing–original draft and figure editing. M.V.H.: Conceptualization; methodology; data curation; formal analysis; writing–review; validation; funding acquisition. J.C.: Conceptualization; methodology; data curation; formal analysis; writing–review; validation; funding acquisition. L.C.W.: data curation; writing–review: A.W.A.K.: Funding acquisition; supervision; validation; writing–review and editing. J.M.S.: Conceptualization; methodology; data curation; formal analysis; writing–review; editing; funding acquisition; supervision.

https://doi.org/10.1017/pab.2026.10111 Published online by Cambridge University Press

Competing Interests. The authors declare no competing interests.

Data Availability Statement. All data generated or analyzed during this study, including raw datasets, R scripts for all phylogenetic and metabolic analyses, and the 3D-scanned femur model with associated parameters, are available in the Dryad Digital Repository at: https://doi.org/10.5061/dryad.t1g1jwtfv

Literature Cited

Allan, G. H., P. Cassey, E. P. Snelling, S. K. Maloney, and R. S. Seymour. 2014. Blood flow for bone remodelling correlates with locomotion in living and extinct birds. *Journal of Experimental Biology* **217**:2956–2962.

Araújo, E. V., R. A. M. Bantim, B. Holgado, J. M. Sayão, L. C. Weinschütz, and A. W. A. Kellner. 2023. Osteohistological characterization and ontogeny of *Caiuajara dobruskii* (Pterosauria, Pterodactyloidea, Tapejaridae). *Historical Biology* **36**:1204–1219.

Araújo, E. V. D., J. Cubo, M. V. A Sena, R. A. M. Bantim, L. C. Weinschütz, A. W. A. Kellner, and J. M. Sayão. 2025. Wing bone laminarity in pterosaurs: insights into torsional adaptations for flight evolution. *Anais da Academia Brasileira de Ciências* **97**:e20240540.

Bennett, A. F., and J. A. Ruben. 1979. Endothermy and activity in vertebrates. *Science* **206**:649–654.

Bert, H., H. Woodward, N. Rinder, R. Amiot, J. R. Horner, C. Lécuyer, M. V. A. Sena, and J. Cubo. 2025. Neonatal state and degree of necessity for parental care in *Maiasaura* based on inferred neonatal metabolic rates. *Scientific Reports* **15**:24827.

Bishop, C. M., and P. J. Butler. 1995. Physiological modelling of oxygen consumption in birds during flight. *Journal of Experimental Biology* **198**: 2153–2163.

Block, B. A. 2011. Endothermy in tunas, billfishes, and sharks. *Encyclopedia of fish physiology: from genome to environment*, **3**:1914–1920.

Buchmann, R., B. Holgado, G. Sobral, L. Avilla, and T. Rodrigues. 2021. Quantitative assessment of the vertebral pneumaticity in an anhanguerid pterosaur using micro-CT scanning. *Scientific Reports* **11**:18718.

Bundle, M. W., H. Hoppeler, R. Vock, J. M. Tester, and P. G. Weyand. 1999. High metabolic rates in running birds. *Nature* **397**:31–32.

Chinsamy, A., L. Codorniú, and L. Chiappe. 2008. Developmental growth patterns of the filter-feeder pterosaur, *Pterodaustro guinazui*. *Biology Letters* **4**:282–285.

Ciezarek, A. G., O. G. Osborne, O. N. Shipley, E. J. Brooks, S. R. Tracey, J. D. McAllister, L. D. Gardner, M. J. E. Sternberg, B. Block, and V. Savolainen. 2019. Phylotranscriptomic insights into the diversification of endothermic *Thunnus tunas*. *Molecular Biology and Evolution* **36**:84–96.

Cincotta, A., M. Nicolaï, H. B. N. Campos, M. McNamara, L. D'Alba, M. D. Shawkey, E. E. Kischlat, et al. 2022. Pterosaur melanosomes support signaling functions for early feathers. *Nature* **604**:684–688.

Claessens, L. P., P. M. O'Connor, and D. M. Unwin. 2009. Respiratory evolution facilitated the origin of pterosaur flight and aerial gigantism. *PLoS ONE* **4**:e4497.

Clarke, A., and H. O. Pörtner. 2010. Temperature, metabolic power and the evolution of endothermy. *Biological Reviews* **85**:703–727.

Clemente, C. J., P. C. Withers, and G. G. Thompson. 2009. Metabolic rate and endurance capacity in Australian varanid lizards (Squamata: Varanidae: Varanus). *Biological Journal of the Linnean Society* **97**:664–676.

Cubo, J., and N. E. Jalil. 2019. Bone histology of *Azendohsaurus laaroussii*: implications for the evolution of thermometabolism in Archosauromorpha. *Paleobiology* **45**:317–330.

Cubo, J., N. Le Roy, C. Martinez-Maza, and L. Montes. 2012. Paleohistological estimation of bone growth rate in extinct archosaurs. *Paleobiology* **38**, 335–349.

Cubo, J., M. V. Sena, P. Aubier, G. Houee, P. Claisse, M. G. Faure-Brac, R. Allain, R. C. L. P. Andrade, J. M. Sayão, and G. R. Oliveira. 2020. Were Notosuchia (Pseudosuchia: Crocodylomorpha) warm-blooded? A palaeohistological analysis suggests ectothermy. *Biological Journal of the Linnean Society* **131**:154–162.

Cubo, J., A. Huttenlocker, L. J. Legendre, C. Olivier, and A. de Ricqlès. 2021. Bone histology and thermal physiology. Pp. 757–773 *in* V. de Buffrénil, A. J. de Ricqlès, L., Zylberberg, and K. Padian, eds. *Vertebrate skeletal histology and paleohistology*. CRC Press, Boca Raton, Fla.

Cubo, J., M. V. A. Sena, R. Pellarin, M. G. Faure-Brac, P. Aubier, C. Cheyron, S. Jouve, R. Allain, and N. E. Jalil. 2025. Integrative paleophysiology of the metriorhynchoid *Pelagosaurus typus* (Pseudosuchia, Thalattosuchia). *Anatomical Record* **308**:394–411.

Dawson, R. R., D. J. Field, P. M. Hull, D. K. Zelenitsky, F. Therrien, and H. P. Affek. 2020. Eggshell geochemistry reveals ancestral metabolic thermoregulation in Dinosauria. *Science Advances* **6**:eaax9361.

DeSantis, L. R., A. C. Sharp, B. W. Schubert, M. W. Colbert, S. C. Wallace, and F. E. Grine. 2020. Clarifying relationships between cranial form and function in tapirs, with implications for the dietary ecology of early hominins. *Scientific Reports* **10**:8809.

Edinger, T. 1927. Das Gehirn der Pterosaurier. *Zeitschrift für Anatomie und Entwicklungsgeschichte* **83**:105–112.

Edinger, T. 1941. The brain of Pterodactylus. *American Journal of Science* **239**:665.

Eleutério, L. H. S., R. A. M. Bantim, F. J. Lima, R. C. L. P. Andrade, A. A. F. Saraiva, A. W. A. Kellner, and J. M. Sayão. 2015. Biomechanical and physiological influences on the osteohistological deposition of Anhangueria (Pterosauria, Pterodactyloidea). *Revista Brasileira de Paleontologia* **18**: 403–412.

Evans, D. C. 2006. Nasal cavity homologies and cranial crest function in lambeosaurine dinosaurs. *Paleobiology* **32**:109–125.

Evans, R. M. 1984. Development of thermoregulation in young white pelicans. *Canadian Journal of Zoology* **62**:808–813.

Faure-Brac, M. G., and J. Cubo. 2020. Were the synapsids primitively endotherms? A palaeohistological approach using phylogenetic eigenvector maps. *Philosophical Transactions of the Royal Society B* **375**:20190138.

Faure-Brac, M. G., R. Amiot, C., de Muizon, J. Cubo, and C. Lécuyer. 2022. Combined paleohistological and isotopic inferences of thermometabolism in extinct Neosuchia, using *Goniopholis* and *Dyrosaurus* (Pseudosuchia: Crocodylomorpha) as case studies. *Paleobiology* **48**:302–323.

Faure-Brac, M. G., H. N. Woodward, P. Aubier, and J. Cubo. 2024. On the origins of endothermy in amniotes. *iScience* **27**:109375.

Fernandes, L. A., and C. M. Magalhães-Ribeiro. 2015. Evolution and palaeoenvironment of the Bauru Basin (Upper Cretaceous, Brazil). *Journal of South American Earth Sciences* **61**:71–90.

Fleischle, C., T. Wintrich, and P. M. Sanders, 2018. Quantitative histological models suggest endothermy in plesiosaurs. *PeerJ* **6**:e4955.

Frappell, P. B., and P. J. Butler. 2004. Minimal metabolic rate, what it is, its usefulness, and its relationship to the evolution of endothermy: a brief synopsis. *Physiological and Biochemical Zoology* **77**:865–868.

Gates, T., C. Organ, and L. Zanno. 2016. Bony cranial ornamentation linked to rapid evolution of gigantic theropod dinosaurs. *Nature Communications* **7**: 12931.

Glazier, D. S. 2005. Beyond the "3/4-power law": variation in the intra- and interspecific scaling of metabolic rate in animals. *Biological Reviews* **80**:611–662.

Grady, J. M., B. J. Enquist, E. Dettweiler-Robinson, N. A. Wright, and F. A. Smith. 2014. Evidence for mesothermy in dinosaurs. *Science* **344**:1268–1272.

Grigg, G., J. Nowack, J. E. P. W. Bicudo, N. C. Bal, H. N. Woodward, and R. S. Seymour. 2022. Whole-body endothermy: ancient, homologous and widespread among the ancestors of mammals, birds and crocodylians. *Biological Reviews* **97**:766–801.

Guénard, G., P. Legendre, and P. Peres-Neto. 2013. Phylogenetic eigenvector maps: a framework to model and predict species traits. *Methods in Ecology and Evolution* **4**:1120–1131.

Handrich, Y., R. M., Bevan, J. B. Charrassin, P. J. Butler, K. Ptz, A. J. Woakes, J. Lage, and Y. L. Maho. 1997. Hypothermia in foraging king penguins. *Nature* **388**:64–67.

Hopson, J. A. 1977. Relative brain size and behavior in archosaurian reptiles. *Annual Review of Ecology and Systematics* **8**:429–448.

Hu, Q., T. J. Nelson, E. P. Snelling, and R. S. Seymour. 2018. Femoral bone perfusion through the nutrient foramen during growth and locomotor development of western grey kangaroos (*Macropus fuliginosus*). *Journal of Experimental Biology* **221**:jeb168625.

Hu, Q., T. J. Nelson, and R. S. Seymour. 2020. Bone foramen dimensions and blood flow calculation: best practices. *Journal of Anatomy*, **236**: 357–369.

https://doi.org/10.1017/pab.2026.10111 Published online by Cambridge University Press

Hu, Q., T. J. Nelson, and R. S. Seymour. 2021. Regional femoral bone blood flow rates in laying and non-laying chickens are estimated with fluorescent microspheres. *Journal of Experimental Biology* **224**: jeb242597.

Hu, Q., T. J. Nelson, and R. S. Seymour. 2022. Morphology of the nutrient artery and its foramen in relation to femoral bone perfusion rates of laying and non-laying hens. *Journal of Anatomy* **240**:94–106.

Hu, Q., C. V. Miller, E. P. Snelling, and R. S. Seymour. 2023. Blood flow rates to leg bones of extinct birds indicate high levels of cursorial locomotion. *Paleobiology* **49**: 700–711.

Huttenlocker, A. K., and C. G. Farmer. 2017. Bone microvasculature tracks red blood cell size diminution in Triassic mammal and dinosaur forerunners. *Current Biology* **27**:48–54.

Kellner, A. W. A. 1996. *Description of the braincase of two Early Cretaceous pterosaurs (Pterodactyloidea) from Brazil*. American Museum Novitates, No. 3175. American Museum of Natural History, New York.

Kellner, A. W. A. 2013. A new unusual tapejarid (Pterosauria, Pterodactyloidea) from the Early Cretaceous Romualdo Formation, Araripe Basin, Brazil. *Earth and Environmental Science Transactions of the Royal Society of Edinburgh* **103**:409–421.

Kellner, A. W. A., and D. A. Campos. 2002. The function of the cranial crest and jaws of a unique pterosaur from the Early Cretaceous of Brazil. *Science* **297**, 389–392.

Kellner, A. W. A., X. Wang, H. Tischlinger, D. A. Campos, D.W. Hone, and X. Meng. 2010. The soft tissue of *Jeholopterus* (Pterosauria, Anurognathidae, Batrachognathinae) and the structure of the pterosaur wing membrane. *Proceedings of the Royal Society B* **277**:321–329.

Kellner, A. W. A., T. Rodrigues, F. R. Costa, L. C. Weinschütz, R. G. Figueiredo, G. A. Souza, A. S. Brum, L. H. S. Eleutério, C. W. Mueller, and J. M. Sayão. 2019a. Pterodactyloid pterosaur bones from Cretaceous deposits of the Antarctic Peninsula. *Anais da Academia Brasileira de Ciências* **91**:e20191300.

Kellner, A. W. A., L. C. Weinschütz, B. Holgado, R. A. M. Bantim, and J. M. Sayão. 2019b. A new toothless pterosaur (Pterodactyloidea) from Southern Brazil with insights into the paleoecology of a Cretaceous desert. *Anais da Academia Brasileira de Ciências* **91**(Suppl 2):e20190768.

Knaus, P. L., A. H. van Heteren, J. K. Lungmus, and P. M. Sander. 2021. High blood flow into the femur indicates elevated aerobic capacity in synapsids since the Synapsida-Sauropsida split. *Frontiers in Ecology and Evolution* **9**: 751238.

Legendre, L. J., L. Segalen, and J. Cubo. 2013. Evidence for high bone growth rate in Euparkeria obtained using a new paleohistological inference model for the humerus. *Journal of Vertebrate Paleontology* **33**:1343–1350.

Legendre, L. J., G. Guénard, J. Botha-Brink, and J. Cubo. 2016. Palaeohistological evidence for ancestral high metabolic rate in archosaurs. *Systematic Biology* **65**:989–996.

Maddison, W. P., and D. R. Maddison. 2016. Mesquite: a modular system for evolutionary analysis. http://mesquiteproject.org.

Manzig, P. C., A. W. A. Kellner, L. C. Weinschütz, C. E. Fragoso, C. S. Vega, G. B. Guimarães, A. L. Godoy, J. H. Z. Ricetti, and C. C. de Moura. 2014. Discovery of a rare pterosaur bone bed in a Cretaceous desert with insights on ontogeny and behavior of flying reptiles. *PloS ONE* **9**:e100005.

Martin, E. G., and C. Palmer. 2014. Air space proportion in pterosaur limb bones using computed tomography and its implications for previous estimates of pneumaticity. *PLoS ONE* **9**:e97159.

McNab, B. K. 2002. *The physiological ecology of vertebrates: a view from energetics*. Cornell University Press, Ithaca, N.Y.

Montes, L., N. Le Roy, M. Perret, V. De Buffrenil, J. Castanet, and J. Cubo. 2007. Relationships between bone growth rate, body mass and resting metabolic rate in growing amniotes: a phylogenetic approach. *Biological Journal of the Linnean Society* **92**:63–76.

Mozo, J., Y. Emre, F. Bouillaud, D. Ricquier, and F. Criscuolo. 2005. Thermoregulation: what role for UCPs in mammals and birds? *Bioscience Reports* **25**:227–249.

Naish, D., M. P. Witton, and E. Martin-Silverstone. 2021. Powered flight in hatchling pterosaurs: evidence from wing form and bone strength. *Scientific Reports* **11**:13130.

Newham, E., P. G. Gill, P. Brewer, M. J. Benton, V. Fernandez, N. J. Gostling, D. Haberthür, et al. 2020. Reptile-like physiology in Early Jurassic stem-mammals. *Nature Communications* **11**:5121.

Padian, K., and J. R. Horner. 2002. Typology versus transformation in the origin of birds. *Trends in Ecology and Evolution* **17**:120–124.

Paladino, F. V., M. P. O'Connor, and J. R. Spotila. 1990. Metabolism of leatherback turtles, gigantothermy, and thermoregulation of dinosaurs. *Nature* **344**:858–860.

Pellarin, R., M. V. A. de Araújo Sena, F. Clarac, and J. Cubo. 2025. Elucidating the thermometabolism of *Thalattosuchus superciliosus* (de Blainville) Young, Brignon, Sachs, Hornung, Foffa, Kitson, Johnson and Steel, 2021 (Archosauria: Metriorhynchidae): a paleohistological study. *Comptes Rendus Palevol* **24**:333–344.

Pettersen, A. K., C. R. White, and D. J. Marshall. 2016. Metabolic rate covaries with fitness and the pace of the life history in the field. *Proceedings of the Royal Society B* **283**:20160323.

Pickering, S., E. Creighton, and B. Stevens-Wood. 1992. Flock size and breeding success in flamingos. *Zoo Biology*, **11**:229–234.

Pimiento, C., J. L. Cantalapiedra, K. Shimada, D. J. Field, and J. B. Smaers. 2019. Evolutionary pathways toward gigantism in sharks and rays. *Evolution* **73**:588–599.

Prondvai, E., K. Stein, A. Ősi, and M. P. Sander. 2012. Life history of *Rhamphorhynchus* inferred from bone histology and the diversity of pterosaurian growth strategies. *PLoS ONE* **7**:e31392.

Pyron, R. A., F. T. Burbrink, and J. J. Wiens. 2013. A phylogeny and revised classification of Squamata, including 4161 species of lizards and snakes. *BMC Evolutionary Biology* **13**:93.

R Core Team. 2023. *R: a language and environment for statistical computing*. R Foundation for Statistical Computing, Vienna, Austria. https://www.R-project.org.

Revell, L. J. 2024. phytools 2.0: an updated R ecosystem for phylogenetic comparative methods (and other things). *PeerJ* **12**:e16505.

Romer, A. S. 1956. The early evolution of land vertebrates. *Proceedings of the American Philosophical Society* **100**:157–167.

Rowland, L. A., N. C. Bal, and M. Periasamy. 2015. The role of skeletal-muscle-based thermogenic mechanisms in vertebrate endothermy. *Biological Reviews* **90**:1279–1297.

Schindelin, J., C. T. Rueden, M. C. Hiner, and K. W. Eliceiri. 2015. The ImageJ ecosystem: an open platform for biomedical image analysis. *Molecular Reproduction and Development* **82**:518–529.

Sena, M. V. A., F. C. Montefeltro, T. S. Marinho, M. C. Langer, T. S. Fachini, A. E. P. Pinheiro, A. S. Machado, et al. 2023. The cost of living in Notosuchia (Crocodyliformes, Mesoeucrocodylia). *Palaeogeography, Palaeoclimatology, Palaeoecology* **632**:111855.

Sena, M. V. A., F. C. Montefeltro, T. S. Marinho, M. C. Langer, T. S. Fachini, A. E. Pinheiro, A. S. Machado, et al. 2025a. Revisiting the aerobic capacity of Notosuchia (Crocodyliformes, Mesoeucrocodylia). *Lethaia* **57**:1–8.

Sena, M. V. A., D. F. Voeten, E. Araújo, and J. Cubo. 2025b. Femoral metadiaphyseal and nutrient foramen perfusion suggests comparable maximal metabolic rates in a pterosaur and in a semi-aquatic maniraptoran dinosaur. *PeerJ* **13**, e19806.

Seymour, R. S. 2013. Maximal aerobic and anaerobic power generation in large crocodiles versus mammals: implications for dinosaur gigantothermy. *PLoS One* **8**:e69361.

Seymour, R. S., C. L. Bennett-Stamper, S. D. Johnston, D. R. Carrier, and G. C. Grigg. 2004. Evidence for endothermic ancestors of crocodiles at the stem of archosaur evolution. *Physiological and Biochemical Zoology* **77**:1051–1067.

Seymour, R. S., S. L. Smith, C. R White, D. M. Henderson, and D. Schwarz-Wings. 2012. Blood flow to long bones indicates activity metabolism in mammals, reptiles and dinosaurs. *Proceedings of the Royal Society B* **279**:451.

Seymour, R. S., Q. Hu, E. P. Snelling, and C. R. White. 2019. Interspecific scaling of blood flow rates and arterial sizes in mammals. *Journal of Experimental Biology* **222**:jeb199554.

Steel, L. 2008. The palaeohistology of pterosaur bone: an overview. *Zitteliana B* **28**:109–125.

Stiller, J., S. Feng, A. A. Chowdhury, I. Rivas-González, D.A. Duchêne, Q. Fang, Y. Deng, et al. 2024. Complexity of avian evolution revealed by family-level genomes. *Nature* **629**:851–860.

https://doi.org/10.1017/pab.2026.10111 Published online by Cambridge University Press

Thompson, G. G., and P. C. Withers. 1997. Standard and maximal metabolic rates of goannas (Squamata: Varanidae). *Physiological Zoology* **70**:307–323.

Torres, C. R., J. A. Clarke, J. R. Groenke, M. C. Lamanna, R. D. MacPhee, G. M. Musser, E. M. Roberts, and P. M. O'Connor. 2025. Cretaceous Antarctic bird skull elucidates early avian ecological diversity. *Nature* **638**:146–151.

Unwin, D. M., and D. C. Deeming. 2008. Pterosaur eggshell structure and its implications for pterosaur reproductive biology. *Zitteliana* **B28**:199–207.

Upham, N. S., J. A. Esselstyn, and W. Jetz. 2019. Inferring the mammal tree: species-level sets of phylogenies for questions in ecology, evolution, and conservation. *PLoS Biology* **17**:e3000494.

Varela, L., S. Tambusso, and R. Fariña. 2024. Femora nutrient foramina and aerobic capacity in giant extinct xenarthrans. *PeerJ* **12**:e17815.

Vidal, N., and S. B. Hedges. 2005. The phylogeny of squamate reptiles (lizards, snakes, and amphisbaenians) inferred from nine nuclear protein-coding genes. *Comptes Rendus Biologies* **328**:1000–1008.

Villa, A., J. Abella, D. M. Alba, S. Almecija, A. Bolet, G. D. Koufos, F. Knoll, et al. 2018. Revision of *Varanus marathonensis* (Squamata, Varanidae) based on historical and new material: morphology, systematics, and paleobiogeography of the European monitor lizards. *PLoS ONE* **13**:e0207719.

Vullo, R., J. Marugan-Lobon, A. W. A. Kellner, A. D. Buscalioni, B. Gomez, M. De la Fuente, and J. J. Moratalla. 2012. A new crested pterosaur from the Early Cretaceous of Spain: the first European tapejarid (Pterodactyloidea: Azhdarchoidea). *PLoS ONE* **7**:e38900.

Wellnhofer, P. 2008. A short history of pterosaur research. *Zitteliana* **B28**: 7–19.

White, C. R., and R. S. Seymour. 2005. Allometric scaling of mammalian metabolism. *Journal of Experimental Biology* **208**:1611–1619.

Williams, J. B., and B. I. Tieleman. 2005. Physiological adaptation in desert birds. *BioScience* **55**:416–425.

Yang, Z., B. Jiang, M. E. McNamara, S. L. Kearns, M. Pittman, T. G. Kaye, P. J. Orr, X. Xu, and M. J. Benton. 2019. Pterosaur integumentary structures with complex feather-like branching. *Nature Ecology and Evolution* **3**:24–30.

Zhou, C. F., D. Yu, Z. Zhu, and B. Andres. 2022. A new wing skeleton of the Jehol tapejarid *Sinopterus* and its implications for ontogeny and paleoecology of the Tapejaridae. *Scientific Reports* **12**:10159.

Zurano, J. P., F. M. Magalhães, A. E. Asato, G. Silva, C. J. Bidau, D. O. Mesquita, and G. C. Costa. 2019. Cetartiodactyla: updating time-calibrated molecular phylogeny. *Molecular Phylogenetics and Evolution* **133**:256–262.

https://doi.org/10.1017/pab.2026.10111 Published online by Cambridge University Press